Well-log interpretation of gas-hydrate-bearing formations in the JAPEX/JNOC/GSC Mallik 2L-38 gas hydrate research well

M. Miyairi[1], K. Akihisa[2], T. Uchida[1], T.S. Collett[3], and S.R. Dallimore[4]

Miyairi, M., Akihisa, K., Uchida, T., Collett, T.S., and Dallimore, S.R., 1999: Well-log interpretation of gas-hydrate-bearing formations in the JAPEX/JNOC/GSC Mallik 2L-38 gas hydrate research well; in *Scientific Results from JAPEX/JNOC/GSC Mallik 2L-38 Gas Hydrate Research Well, Mackenzie Delta, Northwest Territories, Canada, (ed.) S.R. Dallimore, T. Uchida, and T.S. Collett; Geological Survey of Canada, Bulletin 544, p. 281–293.*

Abstract: Techniques for evaluating subsurface natural gas hydrate were part of the JNOC/GSC/JAPEX joint research project. The physical properties of pure methane hydrate, related to well-log responses, were directly measured and/or calculated based on its physico-chemical properties. A petrophysical model of the pore-filling gas hydrate was built considering the existence of thermally dissociated free gas in the pores of the formation. Tool sensitivity to gas hydrate content was analyzed, and formation resistivity and acoustic transit time were found to show distinct sensitivity. Three practical methods for evaluating gas hydrate content were proposed and were tested to confirm their applicability: 1) the resistivity method, 2) the acoustic-velocity method, and 3) the statistical-inversion-analysis method. The porosity and gas hydrate saturation results calculated from these methods agreed quite well. Thus, reasonable interpretations can be achieved using these methods if the drilling and log measurements are carefully designed, and the zoning and parameter settings are made properly in pore-filling-type gas hydrate occurrences similar to those found in the JAPEX/JNOC/GSC Mallik 2L-38 gas hydrate research well.

Résumé : L'application de techniques destinées à l'évaluation des hydrates de gaz naturel de subsurface faisait partie du projet conjoint de recherche JNOC/CGC/JAPEX. On a étudié et/ou calculé les propriétés physiques de l'hydrate de méthane pur liées aux réponses des diagraphies de forage, sur la base de ses propriétés physico-chimiques. On a élaboré un modèle pétrophysique des hydrates de gaz interstitiels en tenant compte de l'existence de gaz libre dissocié thermiquement dans les pores de la formation. La sensibilité des appareils à la teneur en hydrates de gaz a été analysée et on a trouvé que la résistivité de la formation et le temps du parcours acoustique montraient une sensibilité distincte. Les trois méthodes pratiques que nous proposons pour évaluer la teneur en hydrates de gaz ont été mises à l'essai afin de confirmer leurs possibilités d'application. Il s'agit de méthodes basées sur : (1) la résistivité, (2) la vitesse acoustique et (3) l'analyse d'inversion statistique. Les résultats sur la porosité et la saturation en hydrates de gaz calculés à l'aide de ces méthodes sont relativement cohérents. Par conséquent, les interprétations fondées sur ces méthodes sont acceptables à condition que le forage et les mesures effectuées lors des diagraphies soient conçus avec soin et que la détermination de la zonalité et des paramètres soit exécutée correctement dans des indices d'hydrates de gaz interstitiels semblables à ceux rencontrés dans le puits de recherche sur les hydrates de gaz JAPEX/JNOC/GSC Mallik 2L-38.

[1] JAPEX Research Center, Japan Petroleum Exploration Company, Ltd, 1-2-1 Hamada, Mihama-ku, Chiba 261-0025, Japan
[2] Oil Research Ltd., Sanno 2-1-8-713, Ota-ku, Tokyo, Japan
[3] United States Geological Survey, Denver Federal Center, Box 25046, MS-939, Denver, Colorado 80225, U.S.A.
[4] Geological Survey of Canada, 601 Booth Street, Ottawa, Ontario, Canada K1A 0E8

INTRODUCTION

The analysis of wireline well-log data is believed to be one of the most effective methods used to evaluate gas hydrate content in gas-hydrate-bearing sediments (Pearson et al., 1983; Collett et al., 1984; Collett, 1992, 1998a, b; Lee et al., 1993, 1996; Collett and Wendlandt, 1995; Mathews, 1986). Electrical resistivity and acoustic tools respond to the existence of gas hydrate within a formation due to the fact that gas hydrate is an electrical insulator and a ice-like solid substance. The problem was determining how to use wireline log data for quantitative gas hydrate evaluation. The physical and chemical properties of gas hydrate and its occurrence within sediment needed to be clarified before quantitative analysis could be considered. Because gas hydrate is stable only in high-pressure and low-temperature conditions, insufficient laboratory measurements exist to obtain the relation between log responses and gas-hydrate saturation. As a result, while most formation-matrix and fluid properties can be found in the literature or chart books of logging services companies, similar data are not available for gas-hydrate-bearing formations.

Quantitative gas hydrate log-analysis methods have been investigated and proposed by 1) building petrophysical models of gas-hydrate-bearing formations; 2) analyzing tool sensitivity to gas hydrate contents; and 3) applying theoretical and laboratory studies of gas hydrate to actual well-log data measured in the JAPEX/JNOC/GSC Mallik 2L-38 gas hydrate research well. The procedures and results of these studies are summarized in this paper and a discussion follows on how to determine a suitable method among those proposed.

PETROPHYSICAL MODEL

The petrophysical model consists of mineral and pore-filling materials within the gas-hydrate-bearing formation surrounding the well. Gas hydrate occurs mainly within sedimentary rocks below the permafrost layer and within the deep ocean floor, replacing the initial formation waters in the pore space. The facies of the gas-hydrate-bearing formation vary from porous, clean sand to muddy silt. Gas hydrate also occurs in the form of nodules and veins within low-permeability sediments. Basic components of the petrophysical model were selected considering the field observations shown in Table 1.

Other than at the phase boundary between gas hydrate and free gas, it is still not known whether both gas hydrate and free gas can coexist in nature. In general, however, free-gas saturations are considered negligible within the gas hydrate stability zone. The behaviour of fluid displacement surrounding the well in a gas-hydrate-bearing interval has not been measured or simulated until now. It has been calculated that about one hundred and fifty times the volume of methane gas is generated by dissociating methane hydrate under standard conditions, assuming 80–85% of the gas hydrate cage is occupied by methane gas. Depending on depth, the in situ volume of dissociated gas is estimated to be at most twice that of gas hydrate due to high-pressure conditions (Fig. 1).

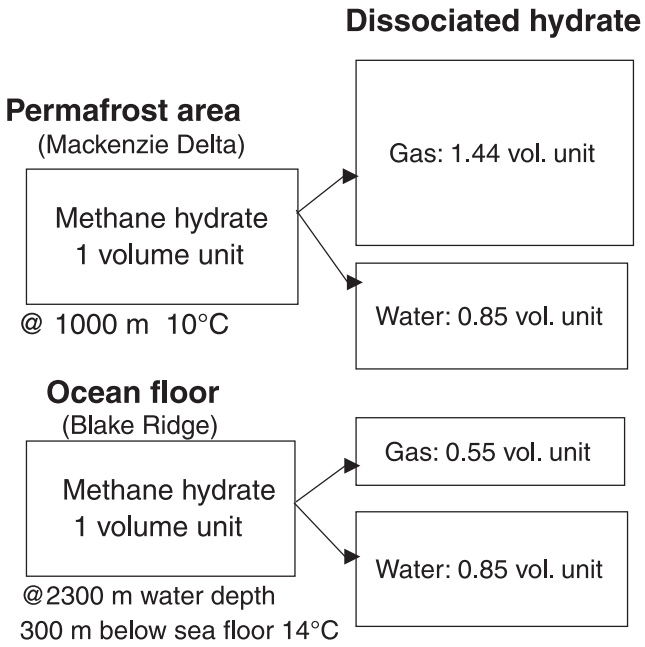

Figure 1. *Comparison of the water and gas content of methane hydrate.*

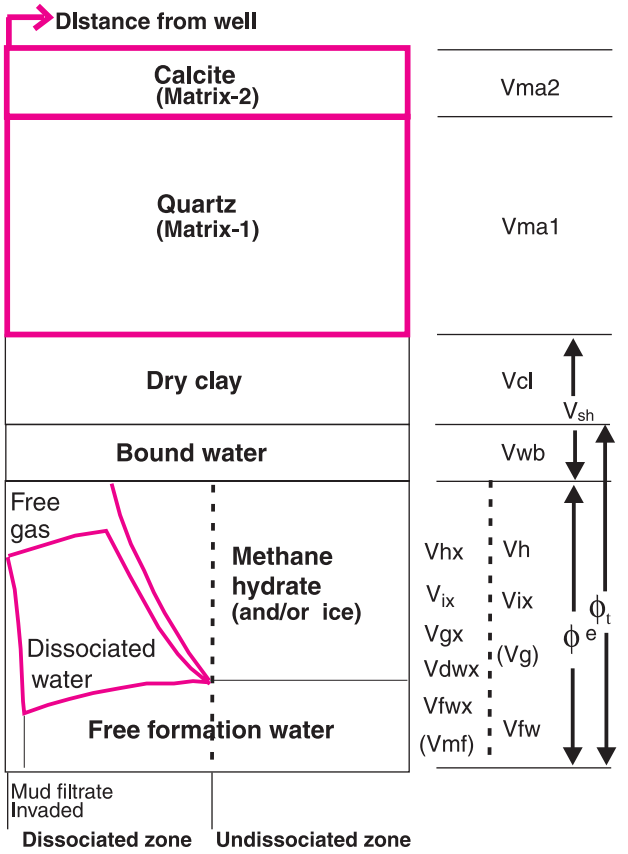

Figure 2. *Petrophysical model of a gas-hydrate-bearing reservoir.*

Figure 2 is the petrophysical model showing the composition and distribution of the matrix and pore-filling components within a gas-hydrate-bearing reservoir.

The physical properties of pure methane hydrate have been investigated in the laboratory by numerous researchers (Davidson, 1973, 1983; Scott et al., 1980; Whalley, 1980; Makogon, 1981; Pandit and King, 1982; Pearson, 1982; Whiffen et al., 1982; Sloan, 1990) and by direct readings from logs from wells that have penetrated massive gas hydrate (Mathews, 1986). These properties were also calculated based on chemical compositions and computer modelling (Collett and Wendlandt, 1995; Collett, 1998b). The results of these studies are summarized in Table 2 together with those of other formation materials.

Table 1. Basic components of the petrophysical model for a gas-hydrate-bearing reservoir.

Typical mineral composition	Pore filling materials	
	Uninvaded zone	Thermally invaded zone
Sandstone (quartz) Calcite cement Clays Bound water	Formation water Gas hydrate Ice (in permafrost)	Mixture of Formation water Dissociated water Mud filtrate Gas hydrate Dissociated methane gas

TOOL-SENSITIVITY ANALYSIS

Tool-sensitivity analysis was carried out using a clean-sand model with a formation-water salinity of 3500 ppm to find effective tools for evaluating gas hydrate saturations. The tools used in this analysis were density, neutron-porosity, acoustic transit-time, and electrical-resistivity logs. The results showed that electrical-resistivity and acoustic transit-time (velocities) logs have significant sensitivity to gas hydrate saturations. Neutron porosity, density, and photoelectric well-log measurements are useful for porosity and lithology calculations due to the minor effect that gas hydrate has on these measurements (Collett, 1998a, 1998b). It was

Table 2. Well-log responses to the typical components of a gas-hydrate-bearing reservoir.

Physical properties	Quartz	Calcite	Shale	Methane hydrate	Ice	Water	Methane gas
Density							
True density, ρ_b (g/cm^3)	2.65	2.71	Variable	0.91	0.92	1.00	Variable
Apparent density, ρ_{log} (g/cm^3)	2.64	2.71	Variable	0.91	0.90	1.00	Variable
Photoelectricity							
Photoelect. absorp., Pe (barn/elect)	1.8	5.1	Variable	0.319	0.358	0.358~0.734	Variable
Vol. Photoelect. Abs., U (barn/cm^3)	4.8	13.8	Variable	0.328	0.371	0.398~0.850	Variable
Neutron							
Epithermal porosity, ϕ N (Lst p.u.)							
Thermal porosity, ϕ N (Lst p.u.)	-2.0	0.0	Variable	106.3	92	100	Variable
Capture. Crossection, Σ (c.u.)	4.3	7.1	Variable	23	20	33	Variable
Thermal decay time, τ (μs)	1058	641	Variable	198	228	138	Variable
Acoustic wave velocity							
Compressional wave							
Velocity, Vp (km/s)	17.9	20.4	Variable	3.3~3.6	3.8	1.5	Variable
Slowness, t (μs/ft)	56.0	49.0	Variable	92.4~84.7	80.2	200	Variable
Shear wave							
Velocity, Vs (km/s)	11.3	11.3	Variable	1.68-1.80	2.00	-	-
Slowness, t (μs/ft)	88.0	88.4	Variable	181-169	152	-	-
Vp/Vs at 272 K	1.58	1.81	Variable		1.90	-	-
Dielectric constant							
Dielectric const., ε (farads/m)	4.65	7.5	Variable	58.0	94.0	59~79	3.0
Electromagn. Prop.time, tp (nsec/m)	7.2	9.1	Variable	25.4	32.3	23~30	6.0
Carbon hydrogen concentration							
Carbon conc., C (atoms/cm ^{3})	0.0E+00	1.626E+22	Variable	4.58E+21	0.0E+00	0.0E+00	Variable
Oxygen conc., O (atoms/cm^3)	5.30E+22	4.88E+22	Variable	2.64E+22	3.1E+22	3.373E+22	-
C/O ratio, COR (fraction)	0.0000	0.3333	Variable	0.1735	0.0000	0.0000	-
Natural gamma-ray, GR (API)			Variable	0	0	0	0
Resistivity, R (ohm-m)	∞	∞	Variable	∞	∞	Variable	∞

barn/elect. – barns/electron
barn/cm^3 – barns/cm^3
Pe – Photoelectric factor (barns/electron)
U – Volumetric photoelectric factor (barns/cm^3)
Lst p.u. – Limestone porosity unit
c.u. – capture unit
prop.time tp – Propagation time of electromagnetic wave
COR – Carbon/Oxygen ratio
API – unit defined by American Petroleum Institute and used as a standard

concluded, therefore, that acoustic transit-time and electrical-resistivity measurements are the best indicators of gas-hydrate saturations.

METHODS TO DERIVE GAS-HYDRATE SATURATIONS

In general, conventional well-log-analysis methods can be used to evaluate formation porosities in gas-hydrate-bearing formations, and these methods can be applied without invoking special techniques (Collett, 1998b). The major problem remains how to estimate gas hydrate content (saturations) within the pore space of a sediment.

Log-analysis methods that were regarded as deserving investigation are shown in Figure 3. In this diagram, each method is classified based on how it calculates gas hydrate saturations (S_h). Among these, the 'resistivity method' and the 'acoustic method' are applied after calculating shale content (V_{sh}) and porosity (ϕ); all unknown values, including V_{sh}, ϕ, and S_h, are analyzed simultaneously in the 'statistical method'. Each of the methods used to calculate gas hydrate saturations are explained in the following section.

Electrical-resistivity method

The electrical-resistivity method uses the Archie equation, or extended versions of the Archie equation, including correction terms for the effect of shale conductivity (e.g. Indonesian equation; Poupon and Leveaux, 1971). In the resistivity method, gas hydrate is regarded as a non-conductive fluid similar to oil and gas.

$$\frac{1}{\sqrt{R_t}} = \left[\frac{V_{sh}^{\,1-V_{sh}/2}}{\sqrt{R_{sh}}} + \frac{\phi^{\,m/2}}{\sqrt{a \cdot R_w}} \right] S_w^{\,n/2} \qquad (1)$$

R_t: formation resistivity (Ω·m)

R_{sh}: shale resistivity (Ω·m)

R_w: formation-water resistivity (Ω·m)

ϕ: porosity (%)

V_{sh}: shale content (%)

S_w: water saturation (%)

a: constant

m: cementation factor

n: saturation exponent

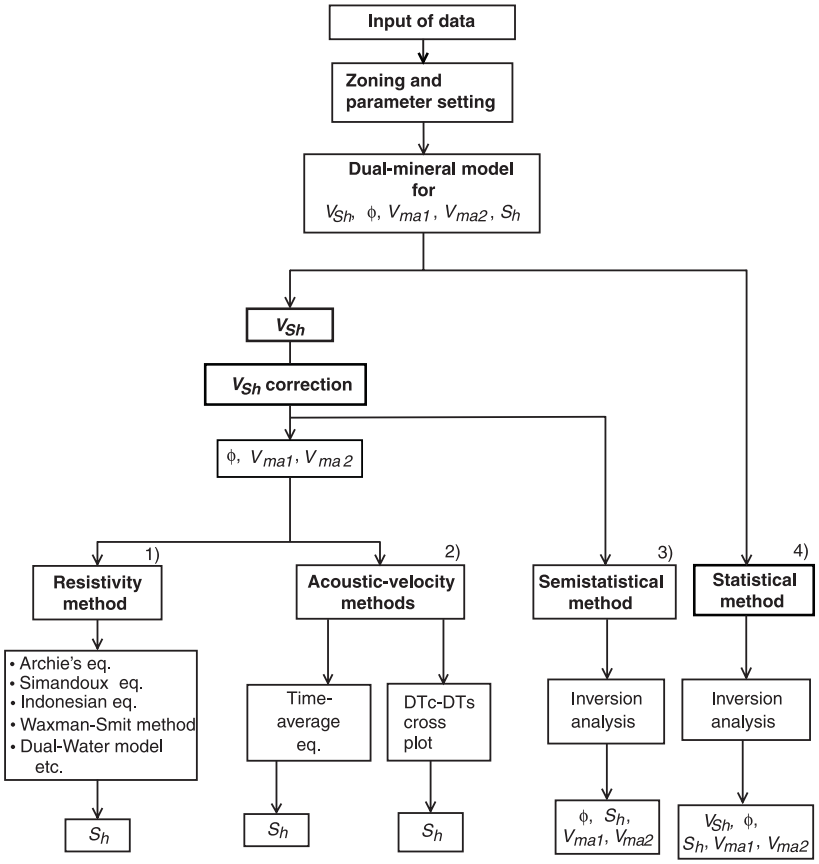

Figure 3.

Well-log analysis methods used to evaluate gas hydrate saturations in the Mallik 2L-38 well.

Acoustic transit-time method

This method is based on a modified Wyllie's equation (reviewed by Collett 1998a). Wyllie's equation can be extended to obtain the following expression so that it can cover the formation of a four-phase model (i.e., grain matrix, shale, fluid/water, gas hydrate) and a compaction factor.

$$t = t_f V_f + t_h V_h + t_{ma} V_{ma} + t_{sh} V_{sh} \quad (2)$$

$$t = t_f \phi(1-S_h) + t_h \phi S_h + t_{ma}(1-\phi-V_{sh}) + t_{sh}\phi V_{sh} \quad (3)$$

$$\phi = \frac{t - t_{ma}}{t_f - t_{ma} - S_h (t_f - t_h)} x \frac{1}{Cp} - V_{sh} \frac{t_{sh} - t_{ma}}{t_f - t_{ma} - S_h (t_f - t_h)} \quad (4)$$

$$S_h = \frac{\phi Cp (t_f - t_{ma}) - t + t_{ma} + V_{sh} Cp (t_{sh} - t_{ma})}{\phi Cp (t_f - t_h)} \quad (5)$$

S_h: gas hydrate saturation (%)

ϕ: porosity (%)

V_{sh}: shale content (%)

V_{ma}: grain-matrix volume (%)

V_f: fluid volume (%)

t: interval acoustic transit time (slowness) (μs/ft)

t_{ma}: slowness of grain matrix (μs/ft)

t_{sh}: slowness of shale (μs/ft)

t_f: slowness of fluid (μs/ft)

t_h: slowness of hydrate (μs/ft)

Cp: compaction factor

The compaction factor is a correction factor for unconsolidated sand, and is usually derived from a cross plot of acoustic- and density-derived porosities.

The time-average equation was first proposed by Wyllie et al. (1958). Timur (1968) proposed a three-phase time-average equation to explain the velocities of compressional waves in consolidated rocks measured at permafrost temperatures. Pearson et al. (1983) applied the equation to gas-hydrate-bearing rock and concluded that it qualitatively explains the known acoustic properties of gas-hydrate-bearing sediment. The above equation is an integrated expression consisting of all major components of the gas-hydrate-bearing formation and the compaction factor.

Statistical inversion method

Each tool responds differently to the various components in the formation (Table 1), and this variable response can be expressed by the following response equation:

$$f_i(\underline{x}) = \sum_{k=1}^{m} e_{ik} X_k \quad \text{for } i = 1, n \quad (6)$$

$f_i(\underline{x})$: theoretical response of tool i

m: number of unknowns (volume of mineral k)

e_{ik}: mineral endpoint of tool i in mineral k

X_k: fractional volume of mineral k

This statistical inversion method applies inversion techniques to derive the volume of each component in the formation. The inversion analysis uses the next incoherence function (Mayer and Sibbit, 1980) to derive an optimum solution:

$$\Delta(\underline{a}, \underline{x}) = \sum_i \frac{[a_i - f_i(\underline{x})]^2}{\sigma_i^2 + \tau_i^2} + \sum_i \frac{g_j(\underline{x})^2}{\tau_j^2} \quad (7)$$

i: kind of tool

a_i: log measurements by tool i

$g_j(\underline{x})$: constraint j

$\underline{x}$: unknowns (e.g., ϕ, S_{xo}, S_w, V_{cl}, V_{ma1}, V_{ma2}, ...)

σ_i: uncertainty on tool i measurement

τ_i: uncertainty on tool i response eq.

τ_j: uncertainty on constraint g_i

The 'semistatistical method' shown in Figure 3 is based on the same logic as the above statistical method. In this method, V_{sh} is evaluated independently beforehand, similarly to how it is determined by the resistivity and acoustic-velocity methods. Shale-corrected, clean equivalent log responses are used for a_i and $f_i(\underline{x})$ in the above equations.

INTERPRETATION OF DOWNHOLE LOG DATA FROM THE MALLIK 2L-38 WELL

The log-interpretation procedures described above were applied to the Mallik 2L-38 gas hydrate research well, drilled on the Mackenzie Delta in February and March, 1998 (Fig. 4). The well location is near that of Mallik L-38, which was drilled by Imperial Oil Limited in 1972 (Dallimore and Collett, 1998; Collett and Dallimore, 1998). The existence of gas hydrate at this site was known by logging and mud-gas records within Oligocene–Miocene sands below the base of permafrost. The previous Mallik L-38 was drilled as a petroleum exploration well and the log quality was poor, especially due to the severe decomposition of in situ gas hydrate during the 22 days before logging.

In Mallik 2L-38, drilling and downhole logging programs were designed to acquire high-quality core and log data. The log data listed in Table 3 are shown as a merged overlay log in Figure 5 together with the mud-gas log. Log interpretations were carried out by utilizing two software packages, 'ALPHA' and 'ELAN Plus', developed by Japan National Oil Corporation (JNOC) (Akihisa et al., 1995, 1996) and Schlumberger, respectively. Both software packages were developed as formation evaluation tools, mainly for petroleum reservoirs. ALPHA was utilized for resistivity,

Table 3. Mallik 2L-38 well-log data used in this study.

Acronym	Units	Log
HDAR	inch	Hole diameter from area
HRLD	Ω·m	High-resolution deep resistivity
HRLS	Ω·m	High-resolution shallow resistivity
RXO8	Ω·m	High-resolution invaded formation resistivity
SP	mV	Spontaneous potential
HGR	GAPI	High-resolution gamma ray
RHO8	g/cc	High-resolution formation bulk density
PEF8		High-resolution formation photoelectric factor
HTNP	v/v	High-resolution thermal neutron porosity (limestone)
DTCO	μ sec/ft	Delta-T (Acoustic transit time) of compressional wave
DTSM	μ sec/ft	Delta-T of shear wave
PR		Poisson shear/compressional ratio

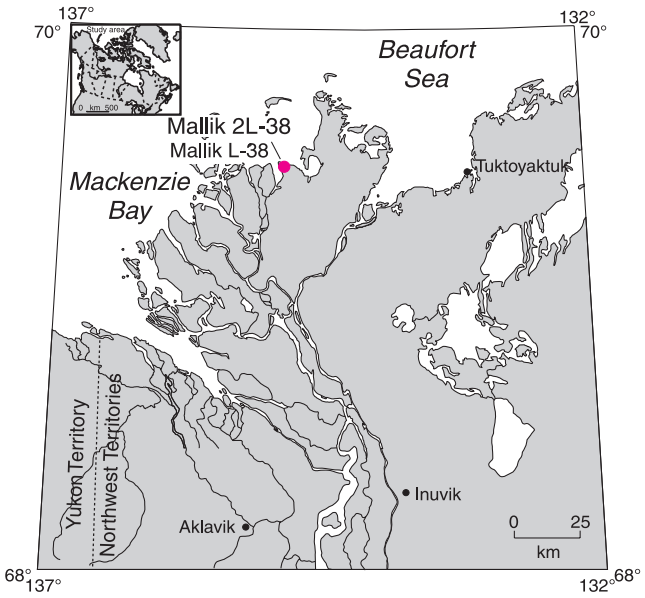

***Figure 4**. Location of the Mallik 2L-38 gas hydrate research well.*

acoustic-velocity and semistatistical approaches by adding special gas hydrate modules. ELAN Plus is equipped with a 'statistical inversion' program, and it was applied to the gas hydrate interval in the Mallik 2L-38 well by setting special 'solve models'.

Overview of downhole log data

Gas-hydrate-bearing intervals are predicted in the composite log display based on log response and mud-gas concentrations (Fig. 5). The gas-hydrate-bearing intervals consist of sand and silty sand beds of the Kugmallit and Mackenzie Bay sequences. Coal and tight sand beds were observed within the cores and exhibited characteristic density and

Table 4. Reservoir and well-log parameters and constants used in this study.

Zone name	Zone I & II	Zone III & IV	Zone V
Depth interval (m.KB)	814-933	933-1076	1076-1150 (TD)
Lithology	Sand and shale	Shaly sand with coal	Shaly sand with coal
Datum level (m.KB)	875	1000	1100
Temperature (°C)	6.9	10.3	13.0
Pore-fluid pressure (psi)	1292	1476	1624
Formation water			
Salinity (ppm)	19000	23500	28000
Density (g/cm^3)	1.023	1.025	1.027
Resistivity Ω·m	0.48	0.38	0.29
Gas			
Compostition	Methane	Methane	Methane
Density (g/cm^3)	0.086	0.099	0.111
Shale response			
Density (g/cm^3)	2.23	2.28	2.28
Vol. photoelectric factor	6.2	6.5	6.5
Neutron porosity (p.u.)	0.38	0.35	0.35
Acoustic slowness (μs/ft)	135	130	130
Resistivity (Ω·m)	5.0	5.0	5.0
KB – kelly bushing			

neutron-porosity log responses. The base of permafrost is estimated at 640 m based on drilling data. It should be noted that all of the depths reported in this paper are well-log depths measured from the kelly bushing (8.31 m above sea level) on the drilling rig used to drill the Mallik 2L-38 well. According to the methane concentrations on the mud-gas log, there seems to be little possibility of significant volumes of gas hydrate within the permafrost interval (0–640 m). In Mallik 2L-38, gas hydrate is inferred to occur in the interval from about 897 to 1110 m. An isolated gas-hydrate-bearing unit at a depth of about 820 m in the Mallik L-38 well was not observed in the Mallik 2L-38 well. Water zones are interpreted below each gas hydrate zone beginning at 897 m, 952 m, 1010 m, and 1075 m, respectively. Such cyclic occurrence of water zones below the gas hydrate intervals would not be observed within the permafrost section.

Representative cross plots of log data are presented in Figure 6. The density-neutron porosity cross plot shows that water-bearing sands and gas-hydrate-bearing sands plot at similar positions, close to the sand line (Fig. 6a); a slight shift toward higher neutron porosities and lower bulk densities is observed for the gas-hydrate-bearing sands. Significant deviation of the plotted 'water-sand' values from the sand line is observed in the acoustic transit-time–neutron-porosity cross plot (Fig. 6b). This deviation is due to the unconsolidated nature of the reservoir sands, and highlights the need for high-compaction correction factors in the time-average equation. The plot of the gas hydrate interval on the density–photoelectric-factor cross plot occurs in an unexpected position between the dolomite and limestone lines due to the effect of barite mud on the photoelectric response (Fig. 6c).

The slowness (or transit time) of shear waves (DTs) shows characteristic behaviour for the gas-hydrate-bearing interval (Fig. 5). At present, the relation between DTs and gas hydrate content is not established, even though a distinct decrease in DTs is observed and is similar to the slowness of compressional waves (DTc) in a gas-hydrate-bearing interval. A cross plot of DTc-DTs implies that a method using a combination of DTc and DTs would be excellent for calculating gas-hydrate saturations (Fig. 6d). Iso-saturation index lines can be drawn in Figure 6d, parallel to plots for water-bearing sand ($S_h = 0\%$), giving a $S_h = 100\%$ line close to the point of maximum distance from the water-sand line.

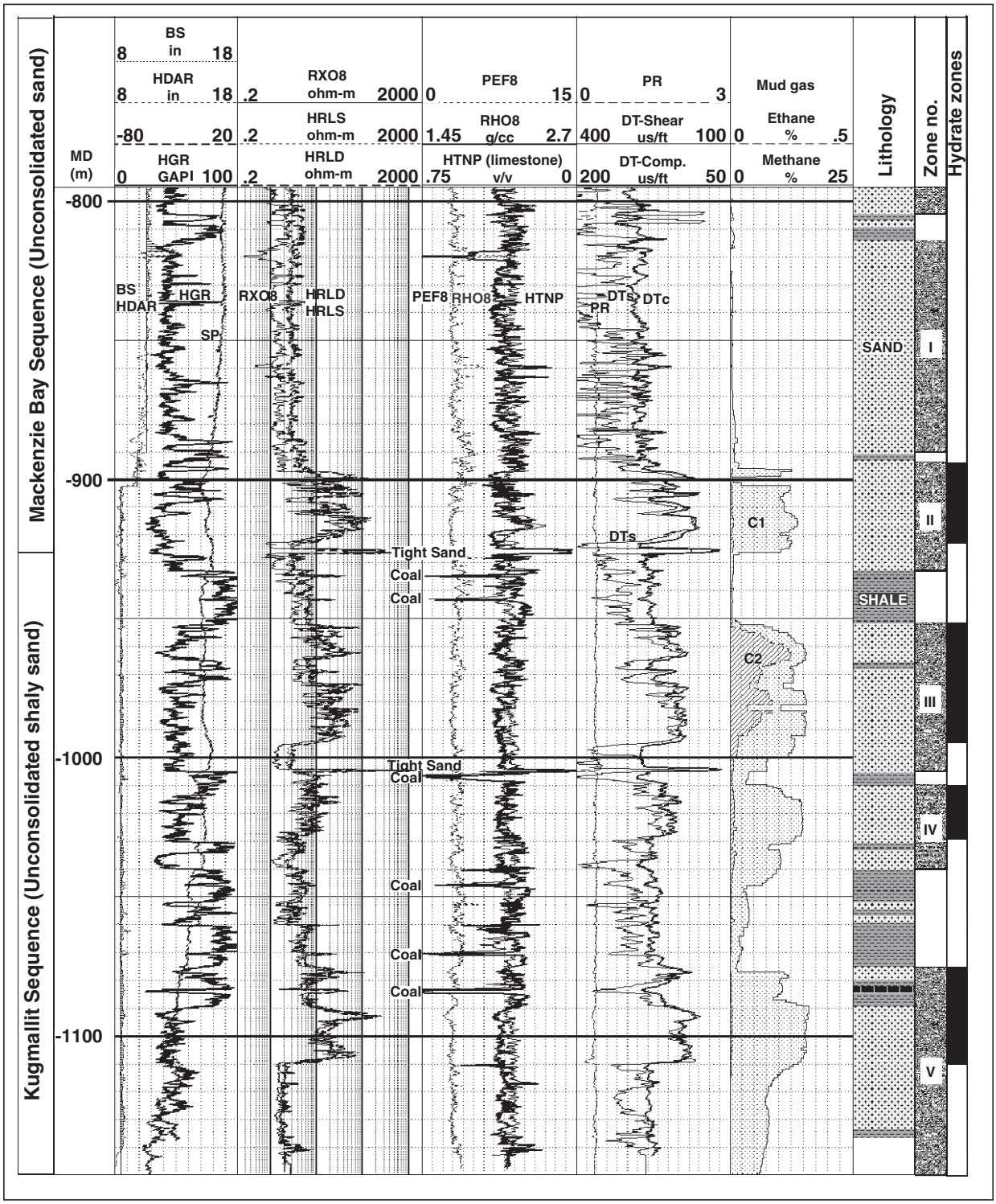

Figure 5. *Downhole well-log data from the gas-hydrate-bearing interval in the Mallik 2L-38 gas hydrate research well. See Table 3 for column-heading definitions.*

Zoning and parameter setting

The well-log-inferred gas-hydrate-bearing interval in the Mallik 2L-38 well was divided into five zones based on lithology and gas hydrate distribution, so that variable reservoir parameters and constants could be assigned for each distinct log-inferred gas hydrate interval (Fig. 5; Table 4). Zones I and II correspond to the Miocene Mackenzie Sequence, while zones III through V are within the Oligocene Kugmallit Sequence. Formation temperatures were estimated assuming a -1°C temperature at the base of the ice-bearing permafrost zone (640 m) and a geothermal gradient of 0.027°C/m (Bily and Dick, 1974). The formation pressure was regarded as equivalent to the hydrostatic condition. The apparent water resistivity (R_{wa}) was calculated to estimate the resistivity of formation water (R_w). The R_{wa} is defined by following equation:

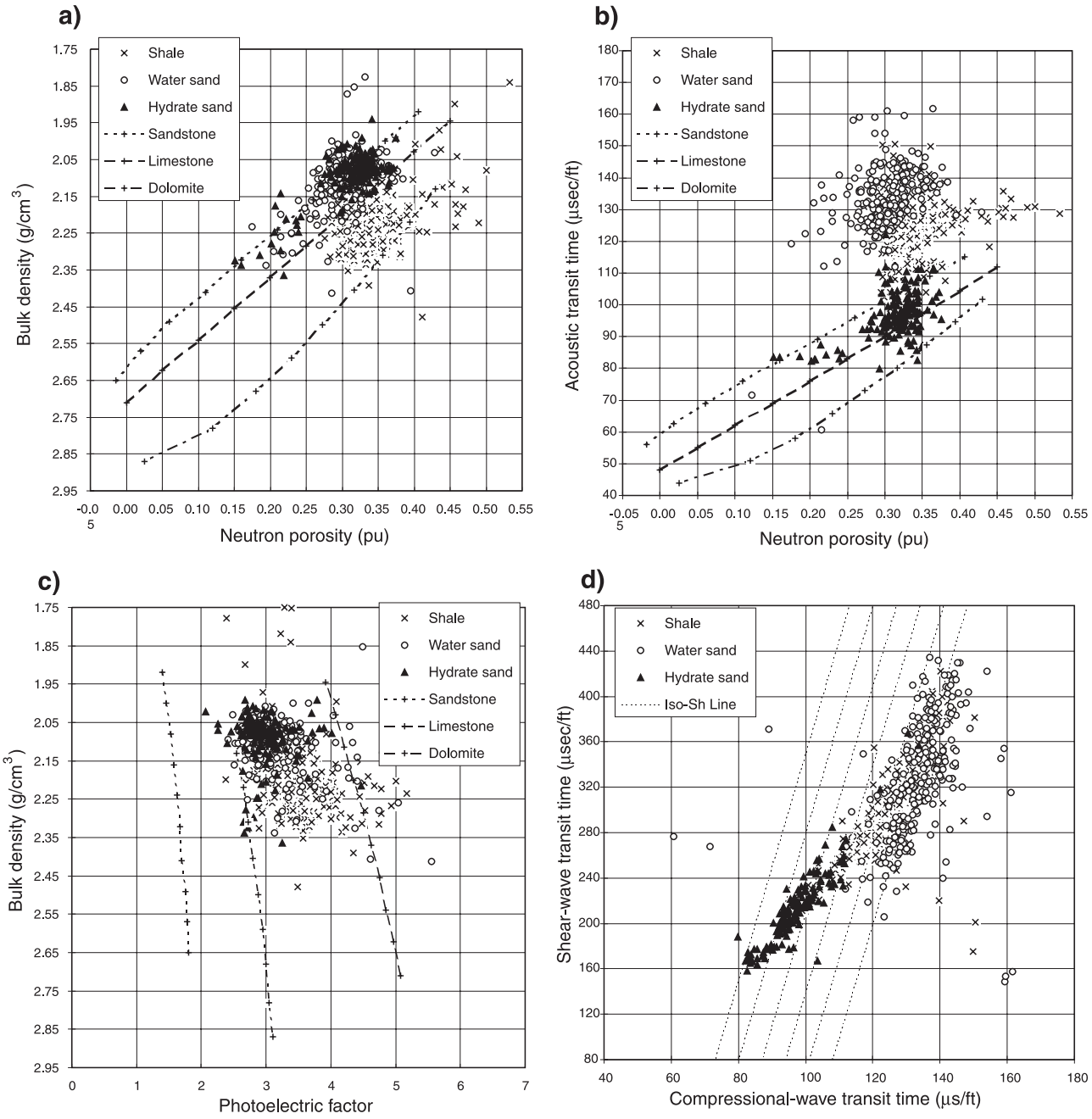

Figure 6. *Cross plots of well-log data from the Mallik 2L-38 gas hydrate research well:* ***a****) density-neutron porosity,* ***b****) acoustic transit-time neutron porosity,* ***c****) density photoelectric factor, and* ***d****) DTcompressional-DTshear.*

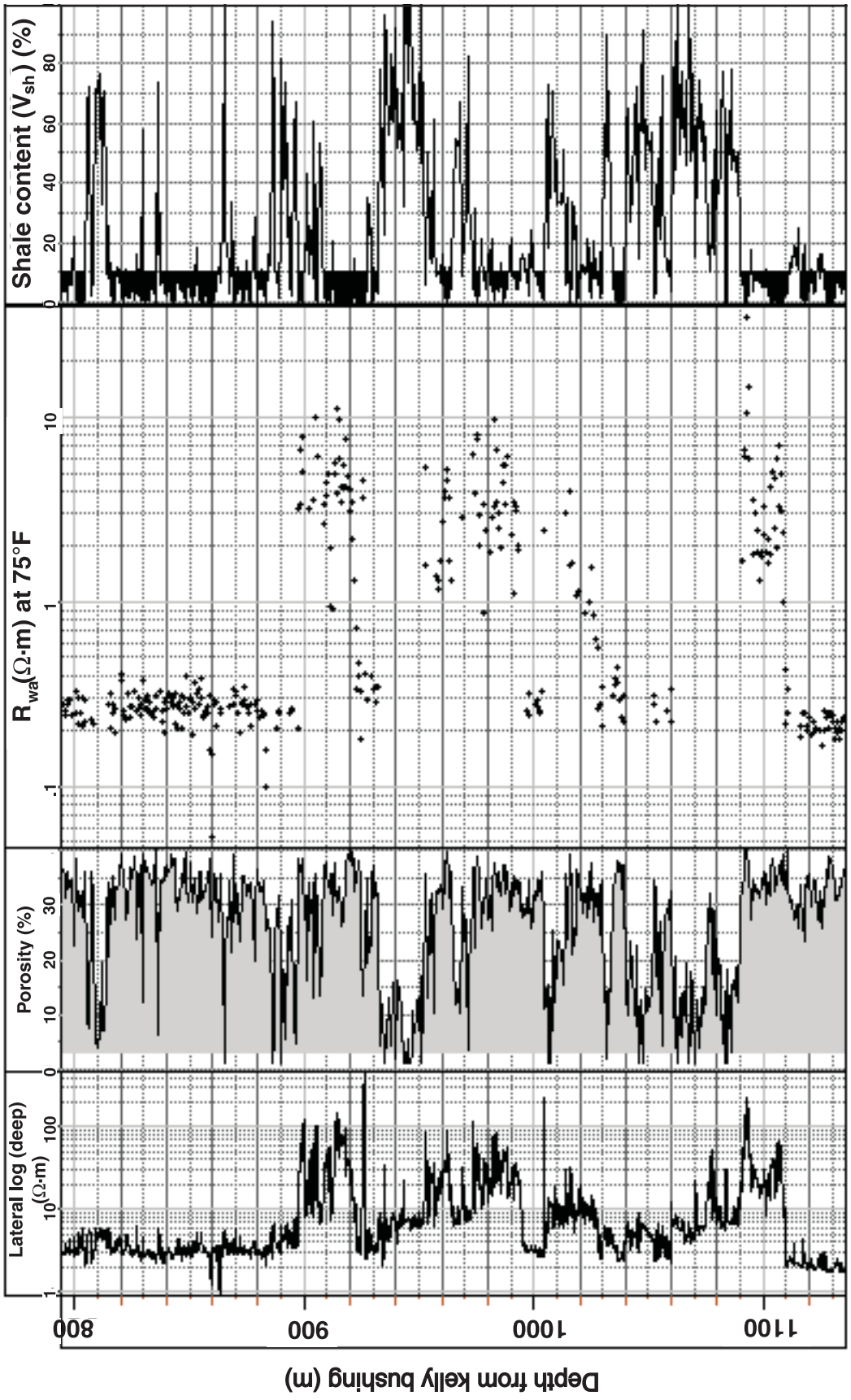

Figure 7. *Well-log-calculated apparent water resistivities (R_{wa}) for the gas-hydrate-bearing interval in the Mallik 2L-38 gas hydrate research well.*

Table 5. Log-analysis methods applied to the interpretation of the Mallik 2L-38 well.

Method	Shale content	Porosity	Hydrate saturation
1) Resistivity	HGR and Clavier eq.	RHO8-HTNP cross plot	Indonesian equation
2) Acoustic velocity	HGR and clavier eq.		Modified time-average equation
ditto	ditto		DTc-DTs cross plot
3) Semistatistical Inversion	HGR and Clavier eq.	Inv. on RHO8/HTNP/DTCO/HRLD/RXOS	
4) Statistical Inversion	Inversion analysis based on RHO8/HTN/DTCO/HGR/HRLD/RXO8		
See Table 3 for definitions			

$$R_{wa} = \frac{R_t}{F} = \frac{R_t \phi^m}{a} \quad (8)$$

The R_{wa} should be equal to the R_w in clean (shale-free) water-bearing formations. The calculated R_{wa} log was characterized by base-line shifts from about 0.4 Ω·m to 0.24 Ω·m with increasing depth (Fig. 7). This implied a salinity change in the formation waters with increasing depth. The salinity and resistivity of the formation waters were determined by Pickett plots for the Zone I aquifer and the bottom of Zone V. The formation-water resistivity of each zone was interpolated as shown in Table 4. Variable shale parameters were determined as shown in Table 4, even though it was difficult to obtain a representative log response, especially within the shallower zones, due to the lack of a massive shale unit.

A compaction factor ranging from 1.40 to 1.55 was determined through the comparison of acoustic-log-derived porosities (ϕ_s) and density-log-derived porosities (ϕ_D) in clean, water-bearing intervals. The acoustic-log-derived porosities (ϕ_s) and density-log-derived porosities (ϕ_D) were calculated with the following equations:

$$\phi_s = \frac{t - t_{ma}}{t_f - t_{ma}} \quad (9)$$

$$\phi_D = \frac{r_{ma} - r_b}{r_{ma} - r_f} \quad (10)$$

As for the parameters in the Archie resistivity equation, standard 'sandstone' values were used: a=0.81, m=2.00, and n=1.75 (assuming an unconsolidated sand). The remaining log-response parameters, used to establish the petrophysical model, are given in Table 2.

Log interpretation

As previously discussed, the interpretation of the log data from the Mallik 2L-38 well was conducted by applying three independent log-analysis procedures: the resistivity method, the acoustic-velocity method, and the statistical-inversion-analysis method and a related 'semistatistical method' (Fig. 3, Table 5). In addition, a DTc-DTs cross-plot method was also used to derive gas hydrate saturations.

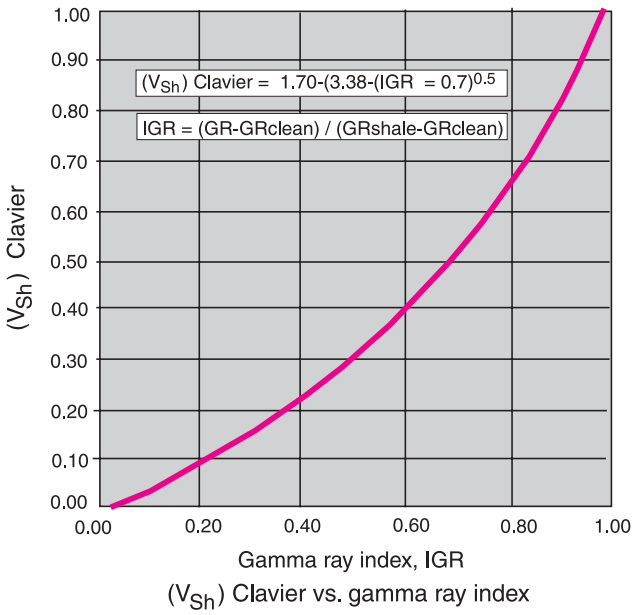

Figure 8. *Graphical display of the Clavier equation used to calculate volume of shale from gamma-ray-log measurements.*

In the first two methods, the gamma-ray log was considered a sufficient shale indicator, as the effects of other radioactive minerals are negligible. The Clavier equation shown in Figure 8 was used to derive shale content (V_{sh}) from the available gamma-ray-log data. The required shale corrections were made for the density, neutron-porosity and acoustic transit time as shown below.

$$\rho_{bc} = \rho_b - \rho_{sh} V_{sh} \quad (11)$$

$$\phi_{Nc} = \phi_N - \phi_{Nsh} V_{sh} \quad (12)$$

$$t_c = t - t_{sh} V_{sh} \quad (13)$$

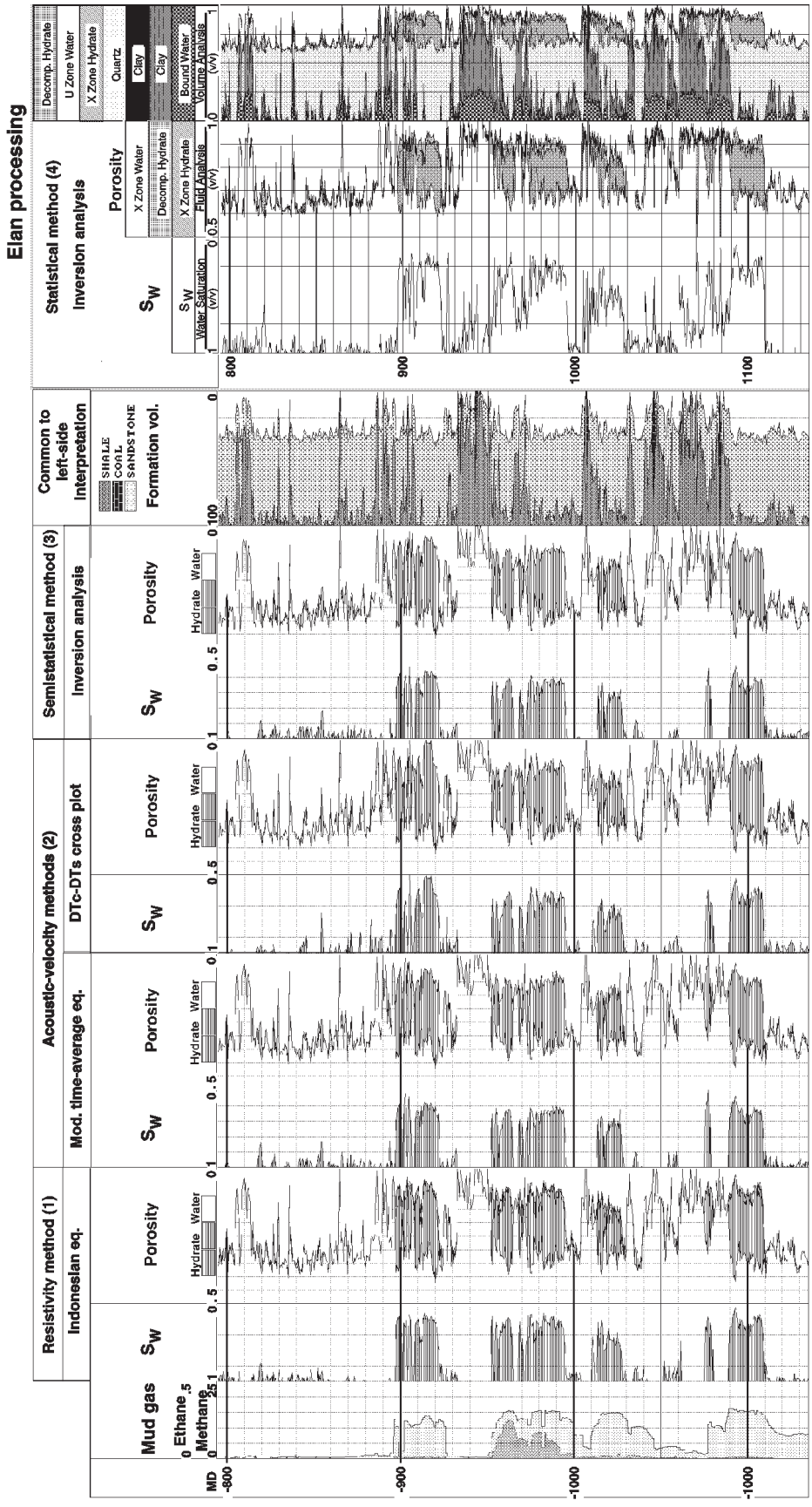

Figure 9. *Comparison of well-log-derived sediment porosities and water saturations (Sw) [gas-hydrate saturations (Sh) = 1-Sw] for the gas-hydrate-bearing interval in the Mallik 2L-38 gas hydrate research well.*

For the resistivity and acoustic-velocity gas-hydrate saturation methods, sediment porosities were derived from a combination of density and neutron logs through the use of shale-corrected log responses. In the semistatistical method, the sediment porosity and water saturations were derived from shale-corrected porosity logs and the resistivity log simultaneously, by using statistical-inversion analysis. In the full statistical method, porosity, shale volume (V_{sh}), water saturation, and gas hydrate saturation were derived from all available logs simultaneously, by using statistical-inversion analysis. Photoelectric data were excluded from the interpretation due to the effect of barite mud.

The results of all of the methods used to calculate sediment porosities and gas hydrate saturations show very similar profiles, as depicted in Figure 9.

DISCUSSION AND CONCLUSIONS

Within this study the following quantitative methods were proposed for gas hydrate content evaluation: 1) the resistivity method using the Indonesian equation; 2) the acoustic method using a modified time-average equation and an additional DTc-DTs acoustic cross-plot method; and 3) the semistatistical and full statistical methods.

The proposed quantitative gas hydrate log-evaluation methods were tested by using the downhole log data acquired from the Mallik 2L-38 gas hydrate research well. Reasonable gas hydrate saturation profiles were obtained from each of the proposed methods. As for the porosities, there is no difference among full statistical, semistatistical, and the other more conventional methods. The gas hydrate saturations calculated from each method also agreed quite well with each other. One of the reasons for this was the proper selection of reservoir parameters and constants. The lack of an appreciable free-gas effect on the recorded well-log measurements associated with thermally disturbed gas hydrate also contributed to the high quality of the log data. These result indicated that reasonable gas hydrate saturations can be obtained from downhole well-log measurements if the drilling program is carefully designed to reduce hole stability problems and if appropriate reservoir parameters and constants are selected in the well-log interpretive phase of the project. Each method considered can be characterized as follows:

1. Resistivity method: the electrical resistivity method is regarded as the most simple and was sufficient in this case, where the occurrence of gas hydrate was similar to that of a conventional oil and gas reservoir.
2. Acoustic-velocity method: like the acoustic-velocity method, the modified time-average equation worked very well. The DTc-DTs cross-plot method appeared to yield reasonable gas hydrate saturations; however, further study of the shear-wave behaviour of gas hydrate is needed.
3. Statistical method with inversion analysis: in general, parameter-setting in statistical-analysis methods requires experience and precise understanding of the log-response equation, because all unknown values are designed to be calculated simultaneously. Careless parameter-setting can easily result in an unrealistic solution, and some skill is needed to obtain realistic values. With accurate parameter-setting, however, statistical well-log-analysis methods yield accurate results. The semistatistical method has the advantage of the flexibility to combine both deterministic and statistical methods.

ACKNOWLEDGMENTS

We are indebted to the Geological Survey of Canada and the ongoing research program supported by JNOC and ten oil, gas, and electric companies in Japan. Special thanks to J-S. Vincent and P.J. Kurfurst of GSC Ottawa, A. Nakamura and M. Imazato of JNOC , and T. Ohara of JAPEX Drilling Department who were responsible for carrying out the Mallik 2L-38 drilling program. We are also grateful to all colleagues who participated with us on the Mallik project and especially to T.H. Mroz of the United States Department of Energy at Morgantown, West Virgina, and O. Senoh of JAPEX Exploration Department at Tokyo.

REFERENCES

Akihisa, K., Ishida, H., and Ebato, T.
1996: Development of statistical well log analysis system — case studies of complex lithology formations; *in* Proceedings of 2nd Annual Well Logging Symposium of Japan, paper B, p. 1–8.

Akihisa, K., Sasaki, S., and Nakamizu, M.
1995: "ALPHA" a statistical well log analysis system; *in* Proceedings of 1st Annual Well Logging Symposium of Japan, paper P, p. 1–8.

Bily, C. and Dick, J.W.L.
1974: Naturally occurring gas hydrates in the Mackenzie Delta, Northwest Territories; Bulletin of Canadian Petroleum Geology, v. 22, no. 3, p.340–352.

Collett, T.S.
1992: Well log evaluation of natural gas hydrates; United States Geological Survey, Open File Report 92-381, 28 p.
1998a: Well log evaluation of gas hydrate saturations; *in* Transactions of the Society of Professional Well Log Analysts, Thirty-Ninth Annual Logging Symposium, 1998, Keystone, Colorado, Paper MM, p.1–28.
1998b: Well log characterization of sediment porosities in gas-hydrate-bearing reservoirs; *in* Proceedings of the 1998 Annual Technical Conference and Exhibition of the Society of Petroleum Engineers, 1998, New Orleans, Louisiana, 12 p.

Collett, T.S. and Dallimore, S.R.
1998: Quantitative assessment of gas hydrates in the Mallik L-38 well, Mackenzie Delta, N.W.T., Canada; *in* Proceedings of the Eighth International Conference on Permafrost, Collection Nordicana, Université Laval, p. 189–194.

Collett, T.S. and Wendlandt, R.F.
1995: Recent developments in well log evaluation of natural gas hydrates; *in* Proceedings of a Conference on Drilling Hydrates in Offshore Japan, (ed.) E.D. Sloan; Center for Hydrate Research, Colorado School of Mines, p. 133–151.

Collett, T.S., Godbole, S.P., and Economides, C.E.
1984: Quantification of in-situ gas hydrates with well logs; *in* Proceedings of the 35th Annual Technical Meeting of the Petroleum Society of CIM, Calgary, Alberta, p.571–582.

Dallimore, S.R. and Collett, T.S.
1998: Gas hydrates associated with deep permafrost in the Mackenzie Delta, N.W.T., Canada; Regional Overview: *in* Proceedings of the Eight International Conference on Permafrost Collection Nordicana, Université Laval, p. 201–206.

Davidson, D.W.
1973: Clathrate hydrates; *in* Water: a comprehensive treatise; (ed.) F. Ranks; Plenum, New York, v. 2, p. 115–234.

Davidson, D.W. (cont.)
1983: Gas hydrates as clathrate ices; *in* Natural Gas Hydrates — Properties, Occurrence and Recovery, (ed.) J. Cox; Butterworth, Woburn, Massachusetts, p.1–16.
Lee, M.W., Hutchinson, D.R., Collett, T.S., and Dillon, W.P.
1996: Seismic velocities for hydrate-bearing sediments using weighted equation; Journal of Geophysical Research, v. 101, no. B9, p. 20 347–20 358.
Lee, M.W., Hutchinson, D.R., Dillon, W.P., Miller, J.J., Agena, W.F., and Swift, B.A.
1993: Method of estimating gas hydrates in deep marine sediments; Marine and Petroleum Geology, v. 10, p. 493–506.
Makogon, Y.F.
1981: Hydrates of natural gas; PennWell Books, Tulsa, Oklahoma, 237 p.
Mathews, M.
1986: Logging characteristics of methane hydrate; The Log Analyst, v.27, no.3, p.26–63.
Mayer, C. and Sibbit, A.
1980: Global, a new approach to computer-processed log interpretation; 55th Annual Fall Technical Conference of the Society of Petroleum Engineers of AIME, Dallas, Texas, SPE 9341, 14 p.
Pandit, B.Z. and King, M.S.
1982: Elastic wave velocities of propane gas hydrates; *in* Natural Gas Hydrates — Properties, Occurrence and Recovery, (ed.) J. Cox; Butterworth, Woburn, Massachusetts, p.49–61.
Pearson, C.F.
1982: Physical properties of natural gas hydrate deposits; Los Alamos National Laboratory Report No. LA-9422-MS.
Pearson, C.F., Halleck, P.M., McGire, P.L., Hermers, R.E., and Mathews, M.A.
1983: Natural gas hydrate deposits, a review of in situ properties; *in* Journal of Physical Chemistry, v. 87, no. 21, p.4180–4185.
Poupon, A. and Leveaux, J.
1971: Evaluation of water saturation in shaly formations; Society of Professional Well Log Analysts, Paper O, 15 p.
Scott, M.I., Randolph, P., and Pangborn, J.B.
1980: Assessment of methane hydrates; Institute of Gas Technology, Report No. GRI-79-0070, 80 p.
Sloan, E.D.
1990: Clathrate hydrates of natural gases; Marcel Decker, New York, New York, 641 p.
Timur, A.
1968: Velocity of compressional waves in porous media at permafrost temperature; Geophysics v. 33, p.584–595.
Whalley, E.
1980: Speed of longitudinal sound in clathrate hydrates; Journal of Geophysical Research, v. 85, no. B5, p.2539–2542.
Whiffen, B.A., Caught, H., and Clouted, M.I.
1982: Determination of acoustic velocities in xenon and methane hydrates by brillouin spectroscopy; Geophysical Research Letters, v. 9, no. 6, p. 645–648.
Wyllie, M.R.J., Gregory, A.R., and Cardner, G.H.F.
1958: An experimental investigation of factors affecting elastic wave velocities in porous media; Geophysics, v. 23, p. 459–493.